Weiss & Ďurovič, 1983). The papers published before 1983 use the Pauling model; the later papers are based on the model of Radoslovich (1961) with *trigonal* symmetry of tetrahedral sheets. In all cases, MDO polytypes (§9.2.2.2.3) have been derived systematically: their sets partially overlap with basic polytypes presented by the US or the USSR schools. The OD models allowed the use of unitary descriptive symbols for individual polytypes from which all the relevant symmetries can be determined (Ďurovič & Dornberger-Schiff, 1981) as well as of extended indicative Ramsdell symbols (Weiss & Ďurovič, 1985*b*). The results, including principles for identification of polytypes, have been summarized by Ďurovič (1981).

The main features of polytypes of basic types of hydrous phyllosilicates, of their diffraction patterns and principles for their identification, are given in the following.

9.2.2.3.1.1. *General geometry*

Tetrahedral and octahedral sheets are the fundamental, *two-dimensionally periodic* structural units, common to all hydrous phyllosilicates. Any *tetrahedral sheet* consists of $(Si,Al,Fe^{3+},Ti^{4+})O_4$ tetrahedra joined by their three basal O atoms to form a network with symmetry $P(3)1m$ (Fig. 9.2.2.6*a*). The atomic coordinates can be related either to a hexagonal axial system with a primitive unit mesh and basis vectors $\mathbf{a}_1$, $\mathbf{a}_2$, or to an orthohexagonal system with a *c*-centred unit mesh and basis vectors $\mathbf{a}$, $\mathbf{b}$ ($b = \sqrt{3}a$). Any *octahedral sheet* consists of $M(O,OH)_6$ octahedra with shared edges (Fig. 9.2.2.6*b*), and with cations M most frequently Mg^{2+}, Al^{3+}, Fe^{2+}, Fe^{3+}, but also Li^{+}, Mn^{2+} ($r_M <\sim 0.9$ Å), *etc*. There are three octahedral sites per unit mesh $\mathbf{a}_1, \mathbf{a}_2$. Crystallochemical classification distinguishes between two extreme cases: *trioctahedral* (all three octahedral sites are occupied) and *dioctahedral* (one site is – even statistically – empty). This classification is based on a bulk chemical composition. A classification from the symmetry point of view distinguishes between three cases: *homo-octahedral* [all three octahedral sites are occupied by the same kind of crystallochemical entity, *i.e.* either by the same kind of ion or by a statistical average of different kinds of ions including voids; symmetry of such a sheet is $H(\bar{3})12/m$];* *meso-octahedral* [two octahedral sites are occupied by the same kind of crystallochemical entity, the third by a different one, in an ordered way; symmetry $P(\bar{3})12/m$)]; and *hetero-octahedral* [each octahedral site is occupied by a different crystallochemical entity in an ordered way; symmetry $P(3)12$]. The prefixes homo-, meso-, hetero- can be combined with the prefixes tri-, di-, or used alone (Ďurovič, 1994).

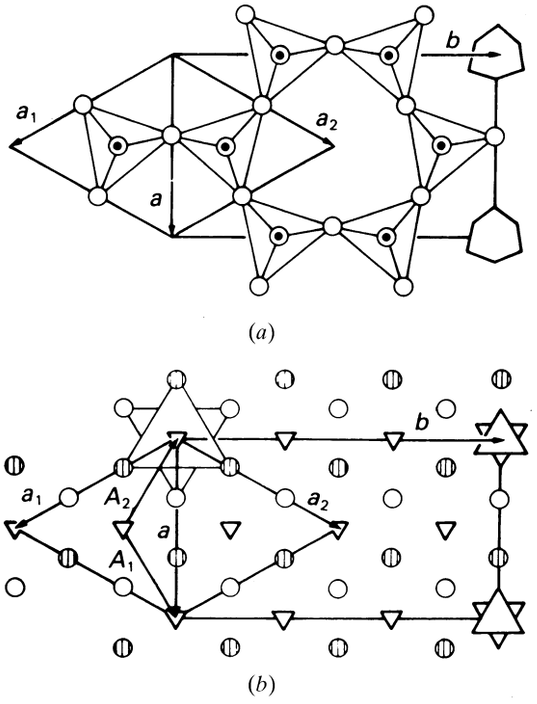

Fig. 9.2.2.6. (*a*) Tetrahedral sheet in a normal projection. Open circles: basal oxygen atoms, circles with black dots: apical oxygen atoms and tetrahedral cations. Hexagonal and orthohexagonal basis vectors and symbolic figures (ditrigons) for pictorial representation of these sheets are also shown. (*b*) Octahedral sheet. Open and shaded circles belong to the lower and the upper oxygen atomic planes, respectively; small triangles denote octahedral sites. Triangular stars on the right are the symbolic figures for pictorial representation of these sheets: the two triangles correspond to the lower and upper basis of any octahedron, respectively.

A tetrahedral sheet (*Tet*) can be combined with an octahedral sheet (*Oc*) either by a shared plane of apical O atoms (in all groups of hydrous phyllosilicates, Fig. 9.2.2.7*a*), or by hydrogen bonds (in the serpentine–kaolin group and in the chlorite group, Fig.9.2.2.7*b*). Two tetrahedral sheets can either form a pair anchored by interlayer cations (in the mica group, Fig. 9.2.2.8*a*) or an unanchored pair (in the talc–pyrophyllite group, Fig. 9.2.2.8*b*).

The ambiguity in the stacking occurs at the centres between adjacent *Tet* and *Oc* and between adjacent *Tet* in the talc–pyrophyllite group. From the solved and refined crystal structures it follows that the displacement of (the origin of) one sheet relative to (the origin of) the adjacent one can only be one (or simultaneously three – for homo-octahedral sheets) of the nine vectors shown in Fig. 9.2.2.9.

The number of possible positions of one sheet relative to the adjacent one can be determined by the corresponding *NFZ* relations (§9.2.2.2.1). As an example, the contact (*Tet*; *Oc*) by shared apical O atoms, and the contacts (*Oc*; *Tet*) by hydrogen

* A hexagonally centred unit mesh $\mathbf{a}_1, \mathbf{a}_2$ instead of a primitive mesh $\mathbf{A}_1, \mathbf{A}_2$ is used (Fig. 9.2.2.6*b*).

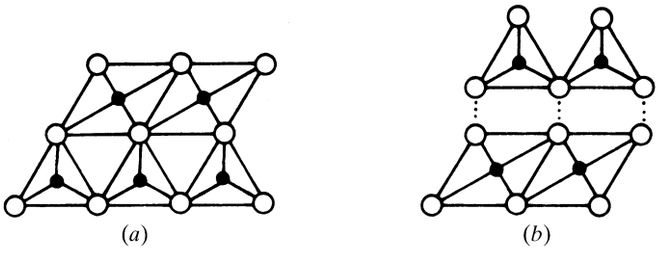

Fig. 9.2.2.7. Two possible combinations of one tetrahedral and one octahedral sheet (*a*) by shared apical O atoms, (*b*) by hydrogen bonds (side projection).

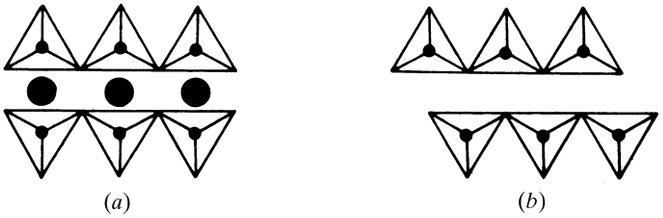

Fig. 9.2.2.8. Combination of two adjacent tetrahedral sheets (*a*) in the mica group, (*b*) in the talc–pyrophyllite group (side projection).

bonds, for a homo-octahedral case, are illustrated in Figs. 9.2.2.10(*a*) and 9.2.2.10(*b*),(*c*), respectively. The two kinds of sheets are represented by the corresponding symbolic figures indicated in Fig. 9.2.2.6. For Fig. 9.2.2.10(*a*): the symmetry of *Tet* is $P(3)1m$, thus $N = 6$; the symmetry of *Oc* is $H(\bar{3})12/m$ and its position relative to *Tet* is such that the symmetry of the pair is $P(3)1m$, thus $F = 6$ and $Z = 1$: this stacking is unambiguous.* But, if the sequence of these two sheets is reversed, $Z = 3$, because $N_{Oc} = 18$ (*h* centring of *Oc*). For Figs. 9.2.2.10(*b*) and (*c*), $Z = 3$. Similar relations can be derived for meso- and hetero-octahedral sheets as well as for the pair (*Tet*; *Tet*) in the talc–pyrophyllite group.

A detailed geometrical analysis shows that the possible positions are always related by vectors $\pm\mathbf{b}/3$. This, together with the trigonal symmetry of the individual sheets, leads to the fact that any superposition structure (§9.2.2.2.5) is trigonal (also rhombohedral) or hexagonal, and the set of diffractions with $k_{\rm ort} \equiv 0 \pmod 3$ has this symmetry too. This is important for the analysis of diffraction patterns.

Some characteristic features of basic types of hydrous phyllosilicates are as follows:

The serpentine–kaolin group: The general structural principle is shown in Fig. 9.2.2.11. The structures belong to category II (§9.2.2.2.7.2). In the homo-octahedral family, there are 12 non-equivalent (16 non-congruent) MDO polytypes (any two polytypes belonging to an enantiomorphous pair are equivalent but not congruent); in the meso-octahedral family, there are 36 non-equivalent (52 non-congruent) MDO polytypes. These sets are identical with the sets of *standard* or *regular* polytypes derived by Bailey (for references see Bailey, 1980) (trioctahedral) and by Zvyagin (1967) (dioctahedral and trioctahedral). The individual polytypes can be ranged into four groups (subfamilies, which are individual OD groupoid families), each with a characteristic superposition structure.

The mica group: The general structural principle is shown in Fig. 9.2.2.12. The structures belong to category IV. There are 6 non-equivalent (8 non-congruent) homo-octahedral MDO polytypes, 14 (22) meso-octahedral, and 36 (60) hetero-octahedral MDO polytypes. The homo-octahedral MDO polytypes are identical with those derived by Smith & Yoder (1956); meso-octahedral MDO polytypes include also those with non-centrosymmetric 2:1 layers (*Tet*; *Oc*; *Tet*); some of these have also been derived by Zvyagin *et al.* (1979). The individual polytypes can be ranged into two groups (subfamilies). For complex polytypes and growth mechanisms, see Baronnet (1975, 1986).

The talc–pyrophyllite group: The general structural principle is shown in Fig. 9.2.2.13. The structures belong to category I. There are 10 (12) MDO polytypes in the talc family (homo-octahedral) and 22 (30) MDO polytypes in the pyrophyllite family (meso-octahedral); some of these have been derived also by Zvyagin *et al.* (1979). The structures can be ranged into two

* If the symmetry of *Tet* is $P(6)mm$ (in the Pauling model), $Z = 2$. This case is common in the literature. However, with the trigonal symmetry of *Tet*, these two possibilities would correspond to Franzini (1969) types *A* and *B*, which are not geometrically equivalent.

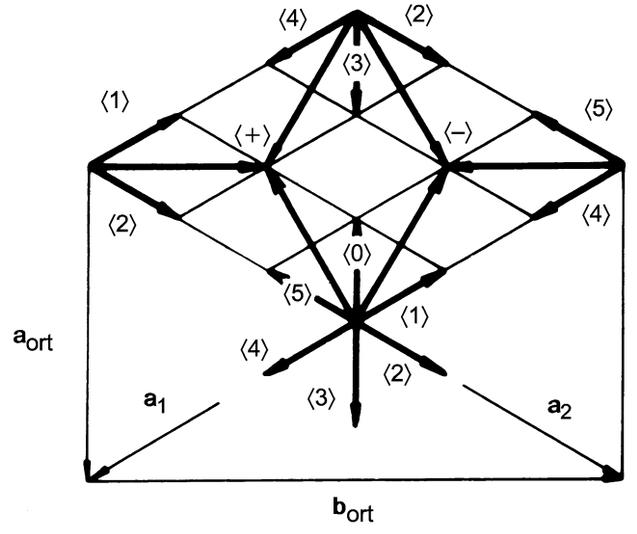

Fig. 9.2.2.9. The nine possible displacements in the structures of polytypes of phyllosilicates. The individual vectors are designated by their conventional numerical characters and the signs +,−. The zero displacement ⟨∗⟩ is not indicated. The relations of these vectors to the basis vectors $\mathbf{a}_1, \mathbf{a}_2$ or $\mathbf{a}, \mathbf{b}$ are evident.

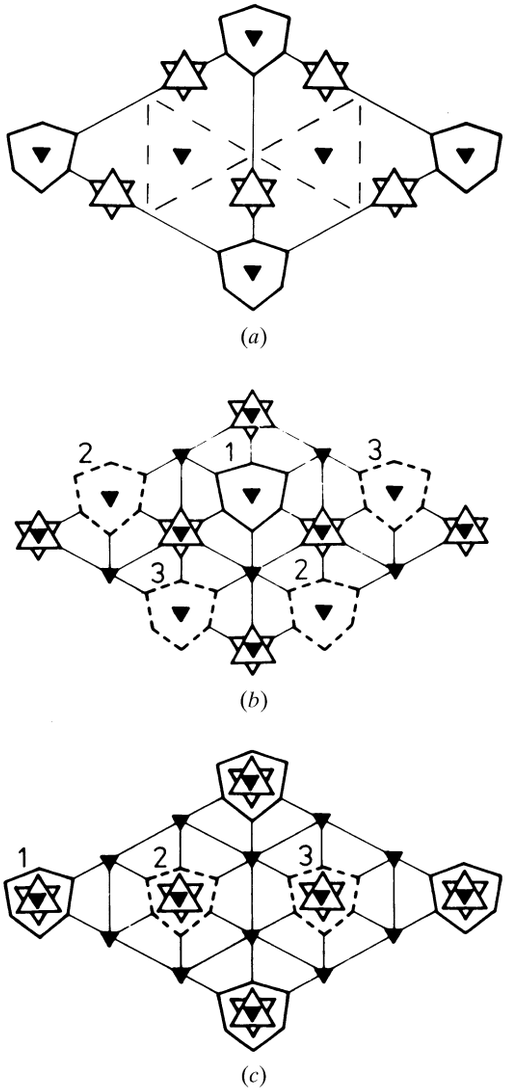

Fig. 9.2.2.10. The *NFZ* relations (*a*) for the pair tetrahedral sheet–homo-octahedral sheet (with shared apical O atoms), (*b*), (*c*) for the pair homo-octahedral sheet–tetrahedral sheet (by hydrogen bonds). The sheets are represented by their symbolic figures; some relevant symmetry elements are also indicated. One of the possible positions (labelled 1) is drawn by full, the other two (2, 3) by broken lines.

groups (subfamilies). For more details, see also Evans & Guggenheim (1988).

The chlorite–vermiculite group: There are two kinds of octahedral sheets in these structures: the *Oc* sandwiched between two *Tet* and the *interlayer* (Fig. 9.2.2.14). The structures belong to category IV. Any *Oc* can be independently homo-, meso-, or hetero-octahedral, and thus, theoretically, there are nine families here. Although vermiculites have a crystal chemistry different from chlorites, they can be, from the symmetry point of view, treated together. There are 20 (24) homo-homo-octahedral, 44 (60) homo-meso-octahedral and 164 (256) meso-meso-octahedral MDO polytypes (the first prefix refers to the 2:1 layer, the second to the interlayer); the other families have not yet been treated. Some of these polytypes have also been derived by other authors (for references, see Bailey, 1980; Zvyagin *et al.*, 1979).

In order to preserve a unitary system, some monoclinic polytypes necessitate a 'third' setting, with the *a* axis unique. These should not be transformed into the standard second setting.

9.2.2.3.1.2. *Diffraction pattern and identification of individual polytypes*

Owing to the trigonal symmetry of the basic structural units and their stacking mode, the single-crystal diffraction pattern of hydrous phyllosilicates has a hexagonal *geometry* and it can be referred to hexagonal or orthohexagonal reciprocal vectors $\mathbf{a}_1^*$, $\mathbf{a}_2^*$ or $\mathbf{a}^*$, $\mathbf{b}^*$, respectively (Figs. 9.2.2.15 and 9.2.2.16). It contains three types of diffractions:

(1) Diffractions 00*l* (or 000*l*), always sharp and common to all polytypes of a family including all its subfamilies. They are indicative of the mineral group, but useless for the identification of polytypes.

(2) The remaining diffractions with $k_{\rm ort} \equiv 0 \pmod 3$, always sharp and common to all polytypes of the same subfamily.

(3) All other diffractions: sharp only for periodic polytypes, otherwise present on diffuse rods parallel to $\mathbf{c}^*$. These are characteristic of individual polytypes. Diffractions 0*kl* – if sharp – are common to all polytypes of the family with the same *bc* projection.

From descriptive geometry, it is known that two orthogonal projections suffice to characterize unambiguously any structure and, therefore, the superposition structure (which implicitly contains the *ac* projection) together with the *bc* projection suffice for an unambiguous characterization of any polytype. It also follows that the diffractions with $k \equiv 0 \pmod 3$ together with the 0*kl* diffractions with $k \not\equiv 0 \pmod 3$ suffice for its determination (except for homometric structures) (Ďurovič, 1981).

From the trigonal or hexagonal symmetry of any superposition structure and from Friedel's law, it follows that the reciprocal rows 20*l*, 13*l*, $\bar{1}3l$, $\bar{2}0l$, $\bar{1}\bar{3}l$, and $1\bar{3}l$ (Fig. 9.2.2.16) carry the same information. Therefore, for identification purposes, it suffices to calculate the distribution of intensities along the reciprocal rows 20*l* (superposition structure – subfamily) and 02*l* (*bc* projection) for all MDO polytypes. Experience shows (Weiss & Ďurovič, 1980) that a mere visual comparison of calculated and observed intensities along these two rows suffices for an unambiguous identification of a MDO polytype. A similar scheme has been presented by Bailey (1988*b*).

The above considerations are based on the ideal Radoslovich model. Diffraction patterns of real structures may exhibit deviations owing to the distortion of the ideal lattice geometry and/or symmetry of the structure.

9.2.2.3.2. *Stibivanite Sb_2VO_5*

The crystal structure of this mineral has been determined by Szymański (1980). It turned out to be identical with that of the compound of the same composition synthesized earlier (Darriet, Bovin & Galy, 1976). The structure is monoclinic with space group $C12/c1$, lattice parameters $a = 17.989\ (6)$, $b = 4.7924\ (7)$, $c = 5.500\ (2)$ Å, $\beta = 95.13\ (3)^\circ$.

Structural units are formed of SbO_2–O–VO–O–SbO_2 extended along **a**, with adjacent units bonded along **c** through Sb—O—Sb and V—O—V bonds. Ribbons are thus formed with no bonding along **b**, and only the Sb—O interactions [2.561 (4) Å] along **a** (Fig. 9.2.2.17). This accounts for the excellent acicular cleavage.

Merlino *et al.* (1989) recognized in this structure sheets of VO_5 square pyramids (*Pyr*) parallel to **bc**, with layer symmetry $P(2/m)2/c2_1/m$ alternating with sheets containing chains of distorted SbO_3 tetrahedron-like pyramids (*Tet*) with layer symmetry $P(1)2_1/c1$ (Fig. 9.2.2.18). Owing to the higher symmetry of *Pyr*, they concluded that there may also exist an alternative attachment of *Tet* to *Pyr*, such that the triples (*Tet*; *Pyr*; *Tet*) will exhibit the layer symmetry $Pmc2_1$, and they will be arranged so that another polytype 2*O* with symmetry $P2_1/m2_1/c2_1/n$ (Fig. 9.2.2.19) is formed [in the original 2*M* polytype, the triples (*Tet*; *Pyr*; *Tet*) have the layer symmetry $P(1)2/c1$]. A mineral with such a structure, with lattice parameters $a = 17.916\ (3)$, $b = 4.700\ (1)$, $c = 5.509\ (1)$ Å, has actually been found.

The polytypism of stibivanite is reflected in its OD character: the two kinds of sheets *Pyr* and *Tet* correspond to two kinds of non-polar layers: their relative position is given by the family symbol:

$$\begin{array}{ll} P(1)2_1/c1 & P(m)cm \\ [1/4, -0.0733\ldots] & \text{category IV,} \end{array}$$

the *NFZ* relations being

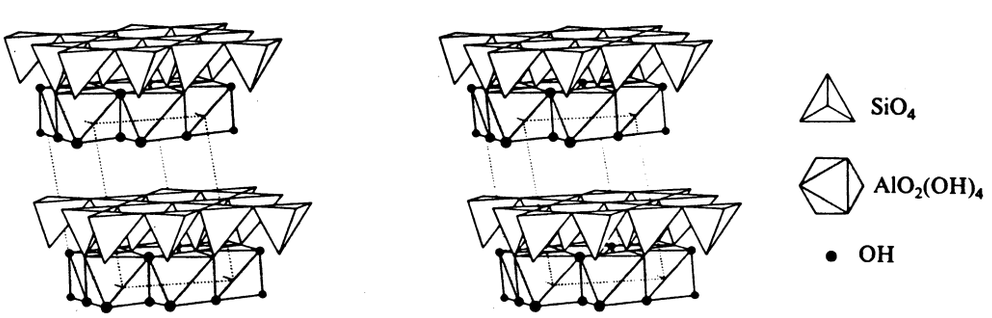

Fig. 9.2.2.11. Stereopair showing the sequence of sheets in the structures of the serpentine–kaolin group (kaolinite-1*A*, courtesy Zoltai & Stout, 1985).